Physical recovery overestimates urban resilience by masking residents' perception dynamics

Zeyu Zhao[1], Jiayu Chen[1], Helen X.H. Bao[*2], Yuhan Zheng[3], Zhaoyi Li[4], John E. Taylor[5], Tianguang Meng*[6], & Dongping Fang[*1]

[1] Department of Construction Management, Tsinghua University, Beijing, China.

[2] Department of Land Economy, University of Cambridge, Cambridge CB3 9EP, UK.

[3] Department of Geography, University of Galway, Galway, Ireland

[4] School of Social and Political Sciences, University of Glasgow, Glasgow, UK

[5]Department of Civil and Environmental Engineering, Georgia Institute of Technology, USA

[6]Department of Political Science, Tsinghua University, Beijing, China

Abstract: With more than half of humanity now concentrated in urban areas, cities have become the primary battleground against the climate crisis, making the resilience in these high-density systems a critical imperative for security. However, conventional resilience prioritizes physical infrastructure metrics, resting on the assumption that technical service restoration equates to societal recovery. This assumption masks a critical disconnect between objective functionality and residents' subjective lived experience. Here, we leverage a catastrophic historic rainstorm as a natural experiment to quantify this "resilience perception gap". By synthesizing millions of geotagged citizen appeals with real-time IoT infrastructure logs, we demonstrate that the gap is not random noise but a structured phenomenon driven by urbanization inequalities and the hierarchy of human needs. Physical metrics systematically overestimate resilience regarding survival necessities (30.2% lag) while underestimating livelihood needs (10.4% surplus). By characterizing these dynamics, we establish the perception gap as a new dimension of urban risk, urging policies that synchronize infrastructure repair with public confidence restoration.

Global climate change and the intensifying frequency of extreme weather events have exposed the fragility of urban systems, making resilience a critical imperative for sustainable development worldwide[1–3]. Historically, resilience assessments have relied on engineering centric paradigms,

prioritizing metrics such as the speed of infrastructure restoration [4,8–10]. However, such physical proxies implicitly assume that technical service restoration equates to societal recovery—an assumption that increasingly fails to capture the lived experience of affected residents[5-7]. This decoupling of physical restoration from perceived recovery creates a critical governance blind spot and inequitable post-disaster resource allocation, exacerbate risking the transformation of natural disasters into prolonged social crises and crises of legitimacy [13,14].

While integrating human perception is recognized as essential, current understanding of the misalignment between physical and perceived recovery remain poorly understood [17]. Emerging empirical studies have documented the existence of this discrepancy, quantifying significant temporal perception lags, such as the 127-day delay in power restoration perception in Puerto Rico after Hurricane María [24] or risk persistence in Zhengzhou[25] and mismatches in resource allocation[11-12,18]. Yet, these studies typically capture only a snapshot of the gap, failing to account for its temporal volatility [19]. They overlook how the gap evolves dynamically as human needs shift hierarchically from survival necessities to long-term livelihood stabilization[20–23]. By treating the gap as a constant rather than a variable structured by urbanization and social capital, current frameworks cannot explain why perception aligns with reality in some phases but sharply diverges in others[15,16]. This leaves the dynamics and drivers of the gap as a black box for urban risk governance. Without decoding these mechanics, policymakers cannot predict when public sentiment will decouple from physical progress, leaving cities vulnerable to secondary social crises.

To bridge this critical knowledge gap, we introduce and operationalize the resilience perception dynamics to decode the structural misalignment between physical and perceived recovery. We posit that this gap is not random noise, but a structured black box governed by the interaction of information asymmetry[29-30], and the hierarchy of human needs[25]. Unlike the static delays observed in prior studies, we hypothesize a non-linear, dynamic trajectory: during the emergency phase, limited cognitive bandwidth leads to an underestimation of disaster impacts (survival prioritization)[31–34]. Conversely, as needs shift to livelihood recovery, anxiety and rising expectations trigger an overestimation of recovery[35-37]. This temporal volatility is further structured by urbanization inequalities: low-urbanized areas face prolonged misalignment due to resource-driven attentional shifts, while high-urbanized regions mask marginalized risk pockets [38-40]. By revealing the specific dynamics and drivers of this misalignment, we expose the perception dynamics where public confidence erodes despite physical progress.

Specifically, this study leverage a natural experiment provided by the July 2023 extreme rainstorm in Beijing, which was a catastrophe that shattered 140-year precipitation records. We tracks the subsequent recovery phase through a massive multi-modal dataset, integrating over

330,000 geotagged citizen service requests, real-time IoT infrastructure logs, and community-level geospatial big data. Spanning 779 communities and impacting 1.31 million residents, this sample covers a urbanization gradient from dense urban cores to mountainous areas, which offers a representation case of megacity resilience challenges. This enables the city-scale, systematic quantification and spatiotemporal deconstruction of the resilience perception gap (Fig. 1). Our dynamic model reveals its predictable temporal evolution and spatial heterogeneity. By integrating the theory of hierarchical human needs into a spatiotemporal big-data analytics framework, we shift resilience assessment from a technocratic exercise to a comprehensive, human-centric paradigm that foregrounds social justice and citizen wellbeing.

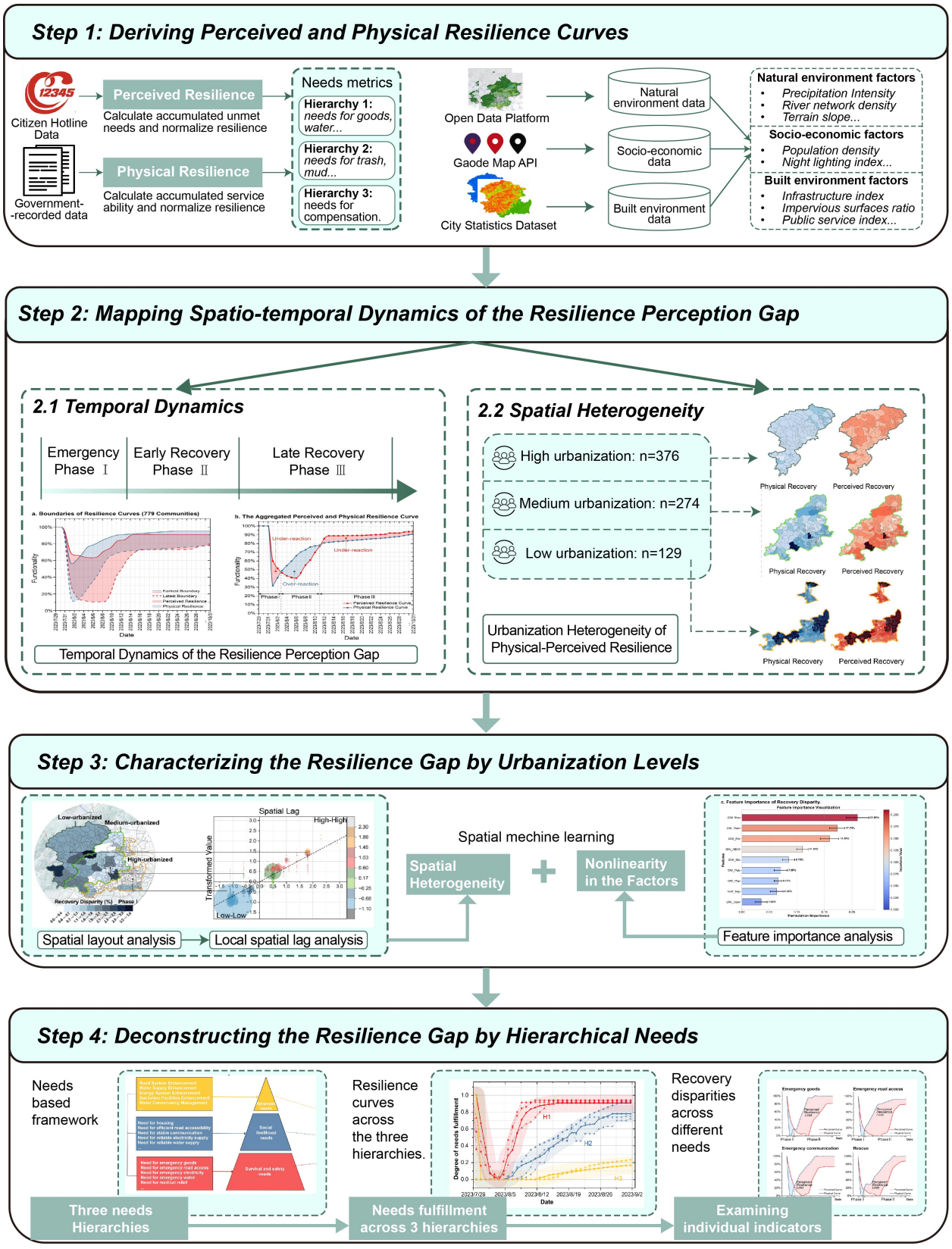
Step 1: Deriving Perceived and Physical Resilience Curves
Citizen Hotline Data
Government--recorded data
Perceived Resilience
Calculate accumulated unmet needs and normalize resilience
Physical Resilience
Calculate accumulated service ability and normalize resilience
Needs metrics
Hierarchy 1: needs for goods, water...
Hierarchy 2: needs for trash, mud...
Hierarchy 3: needs for compensation.
Open Data Platform
Gaode Map API
City Statistics Dataset
Natural environment data
Socio-economic data
Built environment data
Natural environment factors
Precipitation Intensity
River network density
Terrain slope...
Socio-economic factors
Population density
Night lighting index...
Built environment factors
Infrastructure index
Impervious surfaces ratio
Public service index...
Step 2: Mapping Spatio-temporal Dynamics of the Resilience Perception Gap
2.1 Temporal Dynamics
Emergency Phase Ⅰ
Early Recovery Phase Ⅱ
Late Recovery Phase Ⅲ
a. Boundaries of Resilience Curves (779 Communities)
b. The Aggregated Perceived and Physical Resilience Curve
Temporal Dynamics of the Resilience Perception Gap
2.2 Spatial Heterogeneity
High urbanization: n=376
Medium urbanization: n=274
Low urbanization: n=129
Urbanization Heterogeneity of Physical-Perceived Resilience
Physical Recovery
Perceived Recovery
Step 3: Characterizing the Resilience Gap by Urbanization Levels
Low-urbanized
Medium-urbanized
High-urbanized
Spatial Lag
High-High
Low-Low
Transformed Value
Spatial layout analysis
Local spatial lag analysis
Spatial mechine learning
Spatial Heterogeneity
Nonlinearity in the Factors
Feature importance analysis
Step 4: Deconstructing the Resilience Gap by Hierarchical Needs
Needs based framework
Resilience curves across the three hierarchies.
Recovery disparities across different needs
Three needs Hierarchies
Needs fulfillment across 3 hierarchies
Examining individual indicators

Fig. 1|Methodological Workflow. The framework synthesize multi-source data to quantify subjective Perceived versus objective Physical Resilience (Step 1) and map the 'perception gap' across urbanization gradients (Step 2). We then employ spatial machine learning to identify socioeconomic drivers (Step 3) and deconstruct the gap through hierarchical human needs to reveal the recovery inequality (Step 4).

Results

A systemic gap between perceived and physical recovery

We find systematic mismatches characterized by temporal lags and non-overlapping patterns between the physical -perceived recovery curves, (Fig. 2a). Two critical findings emerge: Firstly, both the perceived and physical recovery are defined by an "earliest recovery boundary" (solid line) and "latest recovery boundary" (dashed line), delineating a three-month recovery time window. This temporal framework quantifies the recovery duration observed across communities. Second, the gap between the evolution of the earliest and latest perceived and physical recovery curves is dynamic. The gap between these boundaries widens rapidly in the early stages (0-15 days post-disaster), peaks at 42% recovery disparities, and gradually narrows and stabilizes at 15%. This boundary variation reveals dynamic convergence-divergence patterns: The initial divergence in the early stages highlights the need for rapid and effective communication to manage residents' expectations and address anxieties stemming from potential unmet needs. The subsequent convergence in later stages reflects residents' adaptation to the completion of social and psychological recovery, underscoring the importance of sustained support and interventions to ensure that perceived recovery aligns with physical progress.

Three distinct interaction phases emerge from aggregated curve analysis (Fig. 2b), demonstrating how human risk perception amplifies or attenuates physical recovery signals. The recovery process was categorized into three distinct phases based on the relationship between the residents' subjective perceptions (perceived curves) and the objective restoration of urban functionality (physical curves): preparation and resistance (Phase I), early recovery (Phase II), and late recovery (Phase III).

Phase I: Under-expectation of risk during pre-disaster preparation (July 29th - August 2nd). During this initial phase, perceived recovery exceeded physical recovery by 18% (Δ=+18%), reflecting residents' underestimation of disaster impacts. Pre-disaster overconfidence in urban resilience (from an elderly resident, "In my eighty years here, I've never experienced such a disaster, it won't happen to us.") and delayed recognition of critical infrastructure damage contributed to this perceptual gap. This mismatch may hinder evacuation compliance and preparatory actions, highlighting the need for pre-emptive risk communication strategies to counteract cognitive biases.

Phase II: Over-expectation of risk during emergency restoration (August 3rd-11th). A rapid reversal occurred as physical recovery outpaced perceived recovery by 32% (Δ=-32%), indicating that residents perceive slower recovery than what is objectively occurring. This discrepancy emerges as the post-disaster recovery efforts prioritize infrastructure restoration, such as roads, utilities, and public services, whereas social, psychological, and communication needs remain inadequately addressed. The gap is further exacerbated by persistent fear and uncertainty, as well as limited transparency in recovery planning. This phase underscores the importance of risk communication strategies and community engagement to bridge the perception gap and align public expectations with actual recovery progress.

Phase III: Under-expectation of risk during the long-term recovery stage (August 12th - November 1st). Perceived recovery again surpassed physical recovery (Δ=+12%) as 67% of residents reported adapting to a "new normal", indicating that residents have psychologically adjusted to the recovery outcomes. Despite ongoing infrastructure restoration, the public increasingly perceives the city as "functionally recovered." This shift is influenced by the stabilization of social resilience, the resumption of daily activities, and the development of new behavioral norms post-disaster.

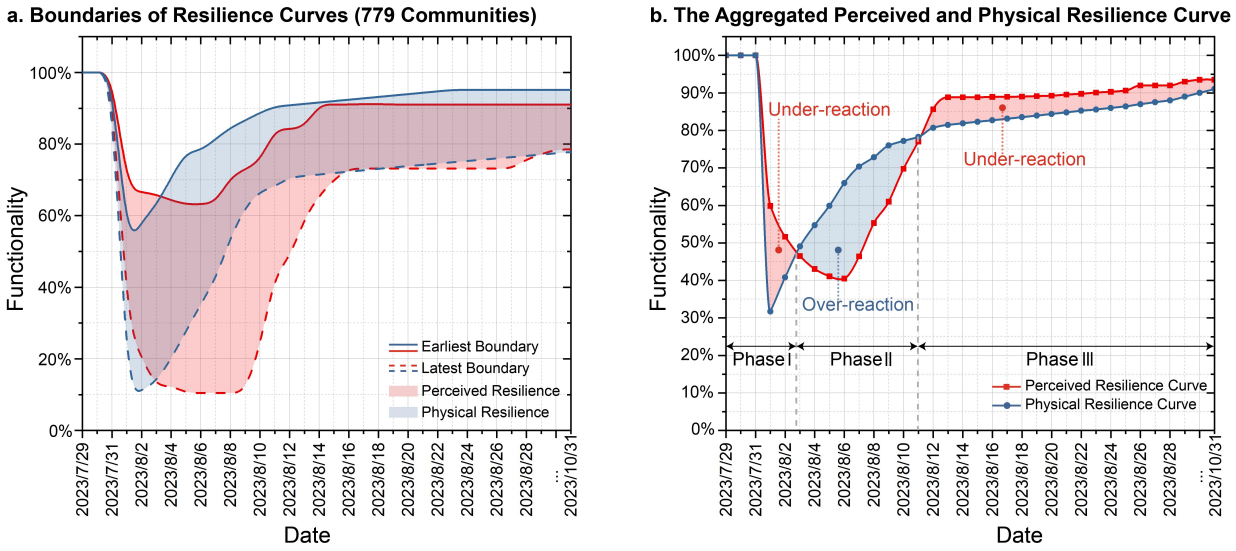

Fig. 2|Temporal Dynamics of the Resilience Perception Gap. a Boundaries of perceived and physical resilience curves across 779 communities (the earliest recovery boundary (solid line) and the latest recovery boundary (dashed line). **b** Aggregated perceived and physical resilience curves, demonstrating overall recovery trends.

Spatial analysis of physical and perceived resilience values across 779 communities reveals systematic misalignments driven by urbanization levels (Fig. 3a-c). This spatial decoupling

quantifies the geography of risk misjudgment. In low-urbanized communities, physical recovery progresses slowly and unevenly, resulting in a persistent divergence between perceived and actual resilience. In contrast, highly urbanized areas exhibit faster and more synchronized recovery, indicating that urban infrastructure, governance efficiency, and resource availability strongly influence how risks and recovery are perceived. To further illustrate the geographic patterns, representative recovery curves from 24 communities (Fig. 3d-f) demonstrate how cognitive-physical gaps propagate through distinct recovery phases.

In low-urbanized communities, disparities between perceived and physical resilience curves peaked at -43.8% on August 8th and persisted for 12 days (Fig. 3d), before perceived resilience surpassed physical resilience from mid-August. This perceptual overshoot (Δ=-43.8%) correlates with underreported infrastructure deficits, exemplifying how limited access to recovery information amplifies risk misjudgment in less urbanized areas. By contrast, medium-urbanized communities demonstrate a moderate perception gap, peaking at −37.3% on August 7, with a 10-day duration before the two curves align by the end of Phase II. This pattern suggests a more balanced recovery process, where infrastructure restoration is gradually recognized by residents, reducing the lag in perception. In high-urbanized communities, the smallest and shortest-lived disparity is observed, with a peak difference of −13.4% on August 6th , lasting only 9 days. The rapid convergence of perceived and physical recovery suggests a well-coordinated response, efficient risk communication, and strong governance, ensuring that residents quickly register actual improvements in urban functionality.

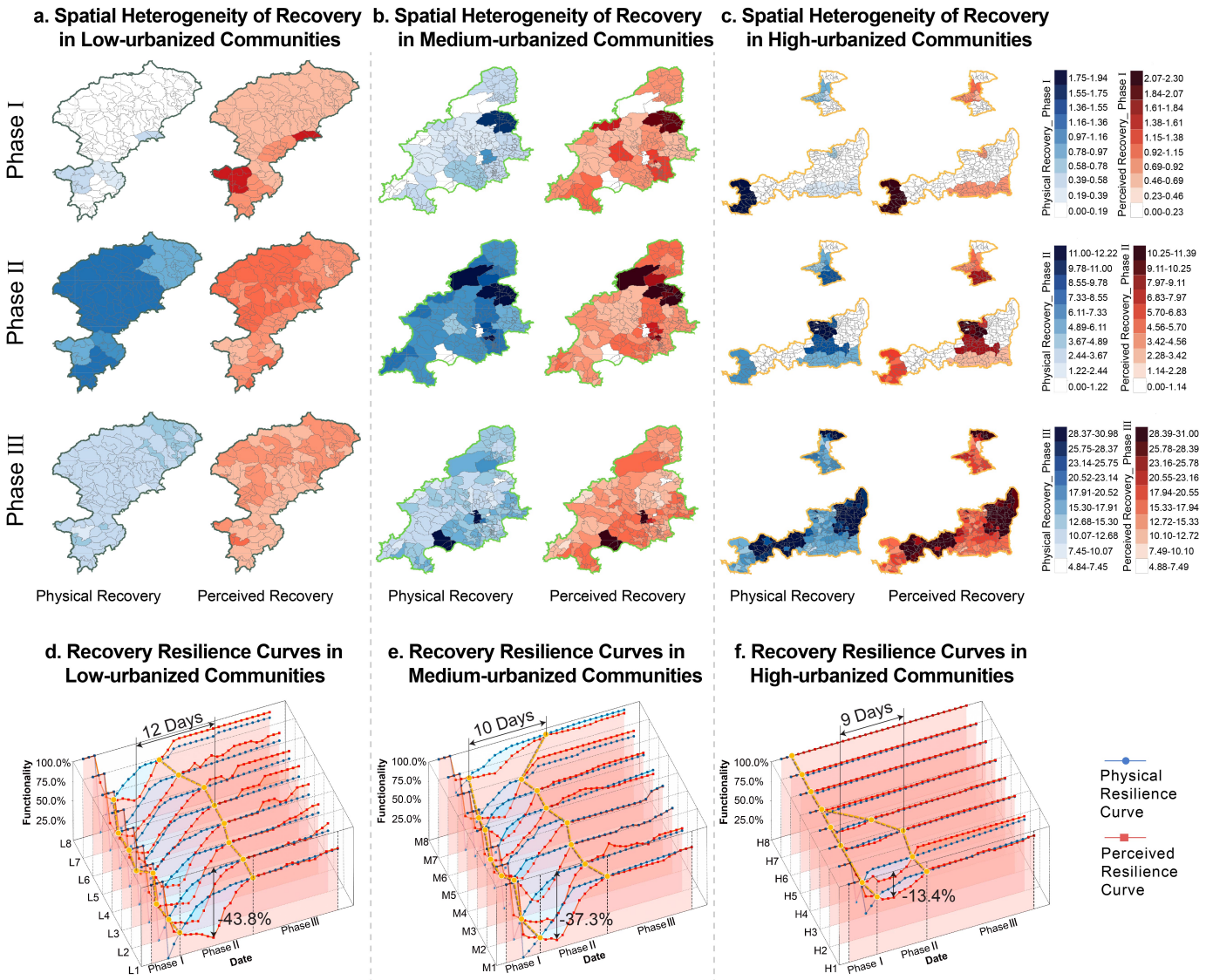

Fig. 3|Urbanization Heterogeneity of Physical-Perceived Recovery Gaps. **a-c** Spatial distributions of physical (left) and perceived (right) resilience values in low- (a), medium- (b), and high-urbanized (c) communities. Warmer colors indicate higher resilience. **d-f** Temporal trajectories of physical (blue) vs. perceived (red) recovery for representative communities: low-urbanized (d), medium-urbanized (e), high-urbanized (f). Shaded areas mark Physical-Perceived gaps.

Spatial Identification and Analysis of the Resilience Perception Gap

The resilience perception gap exhibits marked spatial heterogeneity across the three post-disaster recovery phases (Fig. 4). To characterize this heterogeneity, we quantify gap values for each community, with red regions indicating over-expectation (perceived recovery lags physical recovery) and blue regions denoting under-expectation (perceived recovery exceeds physical recovery).

These spatial patterns dynamically evolve through the recovery process. In Phase I, the under-expectation risk dominated low- and medium-urbanized communities (36% of regions), reflecting residents' delayed recognition of disaster severity. Historical norms and limited access to recovery information likely contributed to this perceptual lag, as evidenced by the delayed mobilization of local response teams in these areas. As recovery progresses into Phase II, a shift occurs towards over-expectation risks. Low-urbanized regions exhibited the most pronounced disparities, where physical recovery progress (e.g., infrastructure repairs) failed to meet residents' escalating expectations (65% of regions). However, this pattern continues in Phase III, with a more varied distribution: under-expectation remains prevalent in low- and medium-urbanized communities, but no misestimations in high -urbanized communities. By Phase III, the disparity landscape becomes more complex: under-expectation persists in low- and medium-urbanized areas, while highly urbanized communities show minimal or no misjudgment in recovery perception.

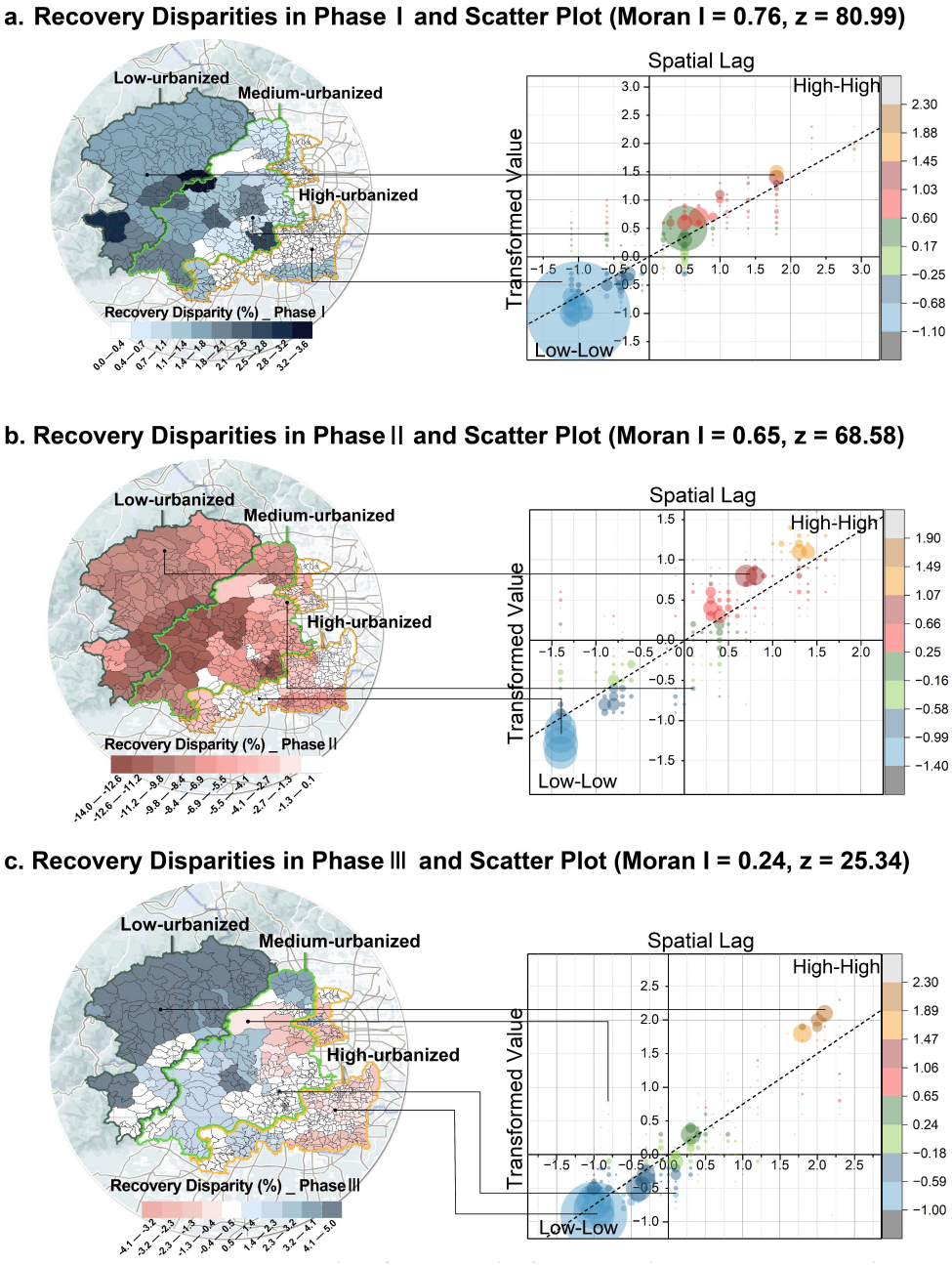

Fig.4|Spatial Heterogeneity of Recovery Disparities Hot-spots. a-c Local spatial auto-correlation: scatter plots of recovery clusters across overall and three phases.

The spatial auto-correlation of recovery disparities further illustrates the changing spatial structure of resilience perception gaps. Across all three phases, values gradually decline, indicating an increase in spatial heterogeneity and a fragmentation of recovery patterns over time. In Phase I, 617 communities exhibit statistically significant spatial auto-correlation, strong spatial autocorrelation ($I = 0.76$, $p < 0.01$) highlighted clustered under-expectation zones in flood-vulnerable communities. In Phase II, reduced clustering ($I = 0.65$,

$p < 0.01$) coincided with emerging outliers, signaling divergent recovery trajectories between neighboring areas. However, Phase II reveals a subtle shift in clustering dynamics, with a wider dispersion of points, particularly in the quadrants. By Phase III, 561 communities maintain significant clustering, weak global autocorrelation ($I = 0.24$, $p < 0.01$) masked localized risk concentrations—14% of high-urbanized communities contained persistent clusters with unresolved infrastructure gaps, while medium-urbanized regions showed expanding boundaries.

Cluster dynamics reveal different risk misjudgment hotspots. In Phase I, large disparities in recovery are found in the most severely affected areas, with high recovery disparities (HH clusters) concentrated in low- and medium-urbanized areas, while low recovery disparities (LL clusters) are concentrated in high-urbanized areas. Moving into Phase II, the spatial pattern remains stable, but there is a noticeable increase in the expansion of mixed recovery clusters (LH and HL). By Phase III, HH clusters decrease and shift towards low-urbanized areas, which begin to show a more balanced recovery. In contrast, LL clusters increase and spread into medium-urbanized regions, where the growth of spatial outliers highlights the growing unevenness of recovery. This growing imbalance between adjacent areas with differing urbanization levels leads to stark contrasts in recovery outcomes. In highly urbanized areas, some pockets of slow recovery persist, pointing to critical areas that require targeted intervention.

Our spatial machine analysis indicates that natural, built environment, and socioeconomic factors exert uneven influences on perceived–physical resilience and their disparities. Among these, rainfall intensity and river network density emerge as the primary drivers in perceived recovery (41.81% importance) and physical recovery (42.55%) but have diminished roles in explaining perceived–physical disparities (17.79%). By contrast, the economic activity index has a more pronounced effect on disparities (21.60%) than on perceived (10.90%) or physical (8.99%) recovery, suggesting that under similar natural conditions, the availability of economic and public resources drives substantial recovery gaps. Moreover, partial dependence plots highlight nonlinear drivers of physical–perceived recovery disparities and their management implications. Certain natural factors show clear thresholds: river density above 0.27/km² yields diminishing returns in reducing disparities; an impervious surface ratio over 0.6 exponentially elevates them; and vegetation coverage (NDVI) beyond 8000 substantially narrows the gap. Overall, natural conditions appear more sensitive to physical outcomes, whereas economic and demographic factors demonstrate threshold-dependent shifts that vary across space. These findings emphasize the importance

of location-specific strategies, particularly targeting resource imbalances that enlarge post-disaster gaps.

Hierarchical needs structure the resilience perception gap

A critical aspect of understanding the risk of misjudging resilience lies in quantifying the disparities between perceived and physical recovery across different hierarchical needs. The goal is not only to diagnose where and when perception gaps emerge but also to inform the redistribution of post-disaster resources to minimize these disparities and enhance overall resilience. To systematically categorize recovery needs, we developed a hierarchical needs framework and identified key post-disaster needs indicators through LDA topic modeling and refined through two Delphi rounds, classified into three hierarchical levels: survival and safety, social livelihood, and advanced long-term needs. The "needs-based functionality curve" (Fig. 5) quantifies these dynamics, where perceived resilience reflects residents' satisfaction with need fulfillment, and physical resilience measures objective resource allocation based on the served population.

This curve represents the degree of need fulfillment over time, based on the degree of needs fulfillment as a proxy. It quantifies the extent to which collective needs are met, computed by aggregating satisfaction levels across all indicators, or alternatively, reverse-coded dissatisfaction scores for unmet needs. For perceived resilience, the degree of needs fulfillment reflects the recovery trajectory of residents' satisfaction levels from accumulated unmet needs. The physical resilience operationalizes as the proportion of residents whose needs are met through resource allocation, reflecting the equilibrium of supply and demand based on the evaluation of government. Notably, both the perceived and physical curves show a sharp decline in needs fulfillment on July 29th, followed by distinct recovery trajectories. When examining the individual needs indicators, differences emerge: for example, the recovery of emergency goods, water, and electricity begins around August 4th in the perceived curve (Fig. 5b) but earlier around August 1st in the physical resilience curve (Fig. 5c). A similar divergence is observed for life-saving needs, including rescue and medical relief. The second hierarchy of needs, such as housing, road accessibility, and utility services (e.g., daily water, power, gas, and sewage systems), exhibits steady improvement during the recovery period. The third hierarchy reflects sustained progress in long-term needs, such as housing reconstruction and infrastructure upgrades, with enhancements anticipated to continue over several years.

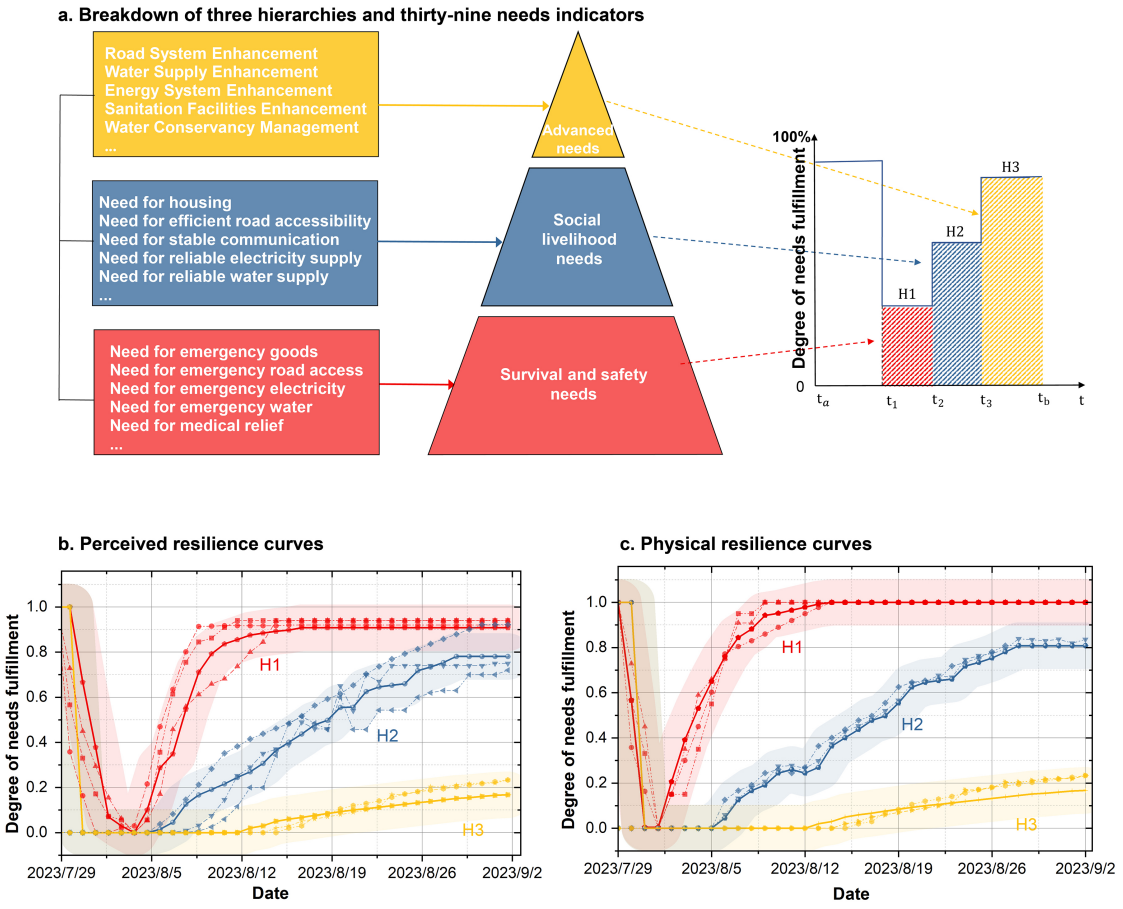

Fig.5|Effects of human needs of three hierarchies. The fulfillment of human needs is analyzed across three hierarchical categories. **a** Breakdown of the three hierarchies, encompassing various needs indicators, illustrating their respective contributions to recovery dynamics. **b** Perceived resilience curves, reflecting subjective recovery trends. **c** Physical resilience curves, demonstrating objective recovery progress across the three hierarchies.

Examining individual indicators reveals notable mismatches.

Survival Needs: Acute Perception Delays. Immediate post-disaster needs (e.g., emergency goods, road access) exhibited severe perceived resilience loss (Δ=30.2 ± 4.1%), where physical recovery outpaced perceptions. For example, emergency communication systems were physically restored by August 1st (*physical resilience*=0.74), yet perceived recovery lagged until August 4th (*perceived resilience*=0.44). This 3-day cognitive latency mirrors residents' heightened sensitivity to unmet survival needs, creating a risk amplification window where distrust in recovery progress escalates despite objective improvements.

Social Livelihood Needs: Misplaced Optimism. Mid-term needs (e.g., housing, utilities) showed an inverted perceived resilience surplus (Δ=+10.4 ± 2.3%). While physical restoration of roads reached 86% (PH=0.86) by Phase II, perceived recovery surged to 94% (perceived resilience=0.94). This overconfidence bias reflects residents' psychological adaptation to partial

progress, masking latent vulnerabilities like drainage overcapacity (*physical resilience*=0.96 vs. *perceived resilience*=0.94). Such mismatches risk premature deprioritization of critical infrastructure investments.

Long-Term Needs: Complacent Alignment. Advanced needs (e.g., housing reconstruction, ecological enhancement) achieved near-perfect perceptual-physical alignment (Δ=+1.2 ± 0.8%), yet high satisfaction scores conceal normalized risk blindness. For instance, while 98% of residents perceived water supply systems as "enhanced" (*perceived resilience*=0.98), physical audits revealed 12% of pipelines remained substandard (*physical resilience*=0.94). This divergence underscores the danger of conflating psychological adaptation with true resilience.

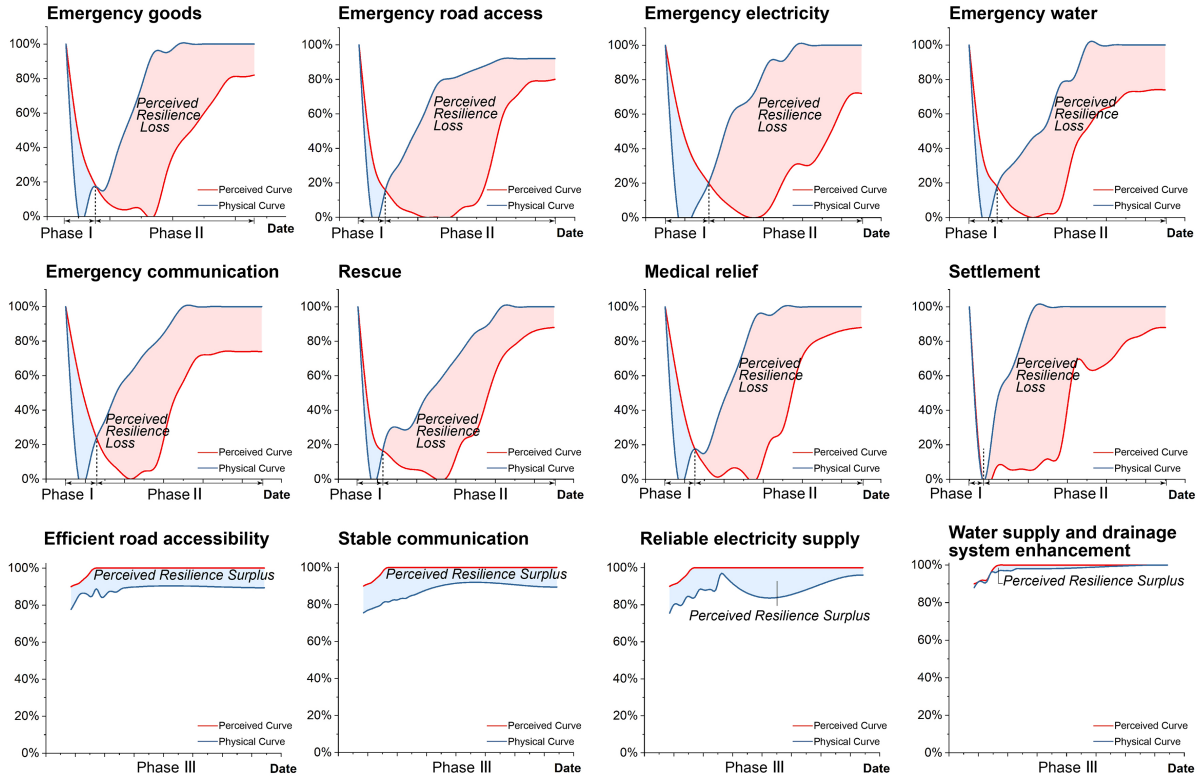

Fig.6|Recovery disparities across different needs. The graphs illustrate perceived (red) and physical (blue) recovery curves for key needs indicators. Notably, the shaded areas include perceived resilience loss in the first hierarchy, with slower perceived recovery compared to physical recovery (e.g., emergency communication and rescue). Conversely, the second and third hierarchies show instances of perceived resilience surplus, where perceived recovery outpaces physical recovery, reflecting an under-expectation to disaster impact.

The harmonization of physical and perceived recovery trajectories serves a critical societal objective: aligning disaster response with residents' expected resilience—the collective standard of recovery shaped by residents' priorities. As quantified in Fig.7, expected resilience thresholds

escalate hierarchically across needs: survival demands rapid but imperfect restoration, social livelihood requires sustained functionality, and long-term needs assume near-perfect recovery. Systematic deviations from these thresholds reveal actionable risk pathways. For immediate survival needs (e.g., emergency goods, road access), both perceived and physical resilience fell critically short of the 0.7 benchmarks during Phase I. Emergency communication systems, for instance, achieved only 44% perceived resilience despite 74% physical restoration, reflecting a 30-percentage-point cognitive lag. This dual deficit—physical progress outpacing trust—explains widespread distrust in early recovery efforts. For social livelihood needs, physical resilience neared the 0.9 benchmarks, yet perceived resilience overshot it. While this perceptual surplus signals restored confidence, it risks complacency—governments may deprioritize investments in systems perceived as "adequately recovered" despite lingering vulnerabilities (e.g., drainage networks operating at 90% capacity). Strategic alignment here involves moderating over-optimism through participatory monitoring of infrastructure performance. Long-term needs achieved nominal alignment with the 1.0 benchmark, yet residual gaps in critical systems like water supply reveal normalized precarity. These deviations, though small, accumulate over time, threatening systemic collapse during subsequent disasters.

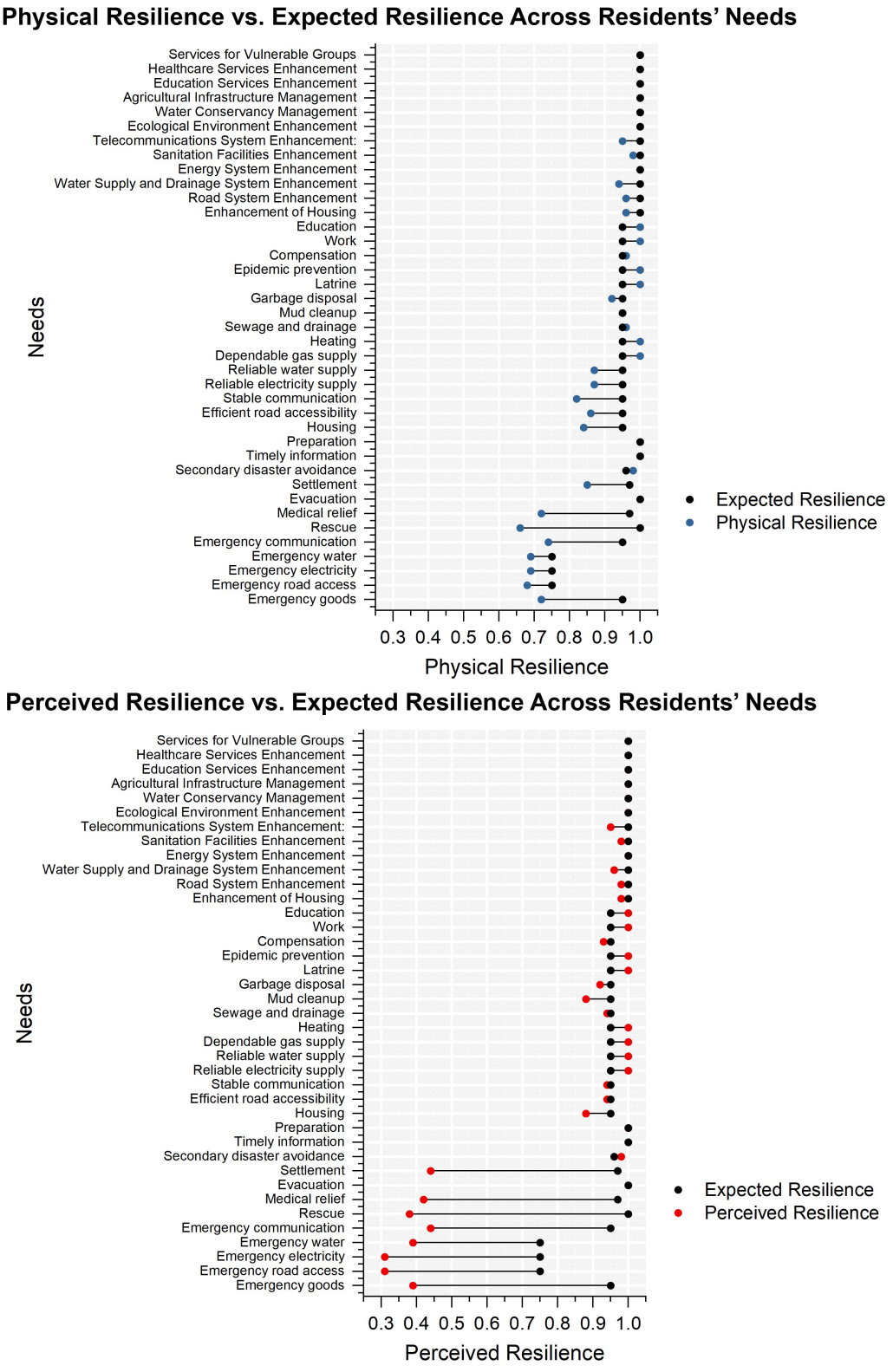

Fig. 7|Expected resilience as a social benchmark for disaster recovery. a Physical resilience (blue points) vs. expected resilience (black points) across survival, social livelihood, and long-term needs. **b** Perceived resilience (red points) vs. expected resilience (black points).

Discussion

This study fundamentally reframes urban resilience by demonstrating that the chasm between a city's physical recovery and its residents' perceived reality is not random noise, but a structured and predictable phenomenon. By defining, quantifying, and mapping the 'resilience perception gap', we introduce a critical and previously invisible dimension of urban vulnerability. Our findings argue that the ultimate success of disaster recovery hinges not solely on the speed of infrastructure repair, but on the successful alignment of this physical progress with human experience.

Residents tend to underestimate disaster impacts in Phase I+ III, but overestimate them in Phase II, which aligns with behavioral theories of risk perception asymmetry[31–33]. Our needs-based framework extends conventional infrastructure-centric resilience metrics by incorporating a Maslowian hierarchy of human requirements, enriching the theoretical foundations of resilience assessment. [21]. The severe perceptual lag in survival needs (Δ=−44%) mirrors COVID-19-era resource misallocations[2], where immediate crises diverted attention from systemic vulnerabilities. Deploying real-time communication platforms[41] to bridge cognitive latency was prone to be important to cities, as tested in flood-prone Latin American communities[42]. For social livelihood needs, perceptual surpluses (Δ=+10%) resemble the "efficiency traps" observed in post-disaster Puerto Rico[34], where rapid visible recovery bred complacency. Implement participatory monitoring, leveraging social capital to balance optimism with accountability[43]. Long-term needs highlight the tyranny of aggregated metrics: near-perfect alignment obscures residual gaps, as seen in unrepaired sewage systems during extreme rainstorms in Beijing [44] and system upgrades in Mianzhu[12].

Urbanization as a Moderator of Risk Pathways: The observed disparities were not across the board, with varying levels of urbanization serving as a proxy. The spatial autocorrelation dynamics (Moran's I: 0.76→0.24) unveil a paradox: while recovery becomes globally heterogeneous, localized risk clusters intensify. Low-urbanized "resilience traps" exhibit cyclical underestimation similar to rural communities[45], where poverty restricts adaptive capacity. Medium-urbanized schism zones mirror fragmented flood responses[46], where competing priorities erode trust. High-urbanized blind spots reflect inequitable flood exposures[35], where aggregate progress masks marginalized groups. These patterns necessitate networked resilience strategies[47], such as cross-city resource sharing[48] and block-level vulnerability indexing[49]. While previous studies have attributed this variation to structural factors such as resource and infrastructure availability [50], our findings highlight the critical role of psychological mechanisms in shaping recovery outcomes. In low-urbanized areas, resource scarcity and poverty significantly influence individual behavior by altering attention focus, prompting individuals to prioritize immediate challenges while neglecting

others[51]. This attentional shift helps explain why residents in these areas focus more on emergency survival needs (e.g., food, water, shelter), reflecting an over-expectation driven by a "short-term priority mindset". However, this focus often leads to neglect of long-term city planning. For instance, residents tend to quickly repair flood barriers based on pre-disaster outdated standards, rather than upgrading infrastructure to reflect contemporary risk factors, inadvertently exacerbating future vulnerabilities. Moreover, emotional distress and poverty-related stress amplify their over-expectation to disaster recovery. In line with existing findings [29,30], this emotional vulnerability, combined with weakened cognitive functions, increases the tendency to engage in risk-averse behavior and discount future risks (time-discounting)[30,51].

Considering these findings jointly, our study explores the interplay between psychological mechanisms and urbanization-related disparities in shaping recovery processes. By linking perception biases such as information asymmetry, cognitive limitations, and anxiety to recovery disparities, our findings expand the current understanding of disaster recovery. Unlike traditional studies that mainly focus on physical infrastructure or resource availability[52], this research introduces a novel understanding that integrates cognitive and perceived dimensions into resilience planning. Recognizing the influence of psychological factors on disaster recovery underscores the need for interventions that address both material and cognitive challenges. This includes developing communication strategies that effectively convey risk information, provide clear guidance during emergencies, and manage expectations throughout the recovery process. It also highlights the importance of incorporating mental health support into disaster preparedness and response plans, particularly for vulnerable populations who may experience heightened anxiety and stress. Policymakers should prioritize investments in early warning systems, risk communication campaigns, and community-based preparedness programs. Practitioners should develop culturally sensitive and accessible resources to address mental health needs during and after disasters.

Three Approaches to Minimize Recovery Disparities and Perceptiobn Biases. (1) The first strategy prioritizes investment in physical restoration to accelerate infrastructural recovery, thereby elevating perceived resilience—though this entails significant fiscal commitments. While such enhancements can align resident perceptions with actual recovery outcomes, surpassing a critical threshold of psychological satisfaction leads to diminishing returns; beyond this point, additional investment yields minimal gains in public confidence. (2) The second approach emphasizes targeted, needs-based interventions to synchronize physical and perceived recovery while optimizing fiscal efficiency. By prioritizing region-specific needs, this strategy enables more precise resource allocation compared to large-scale restoration efforts. For social livelihood recovery, key actions include reestablishing transportation networks, facilitating financial

assistance, and supporting local business rehabilitation. For long-term resilience, investments should focus on infrastructure upgrades, community development programs, and psychosocial support services. (3)The third strategy adopts a non-material approach, focusing on socio-institutional interventions designed to elevate perceived recovery and reinforce social stability—requiring minimal fiscal expenditure while relying on behavioral and communicative mechanisms. Through strategic communication and institutional signaling, authorities can directly shape residents' perception of recovery progress. This emphasis on socio-perceptual dimensions complements physical reconstruction efforts by addressing psychological and behavioral determinants of resilience, thereby reducing recovery disparities without substantial capital investment.

Limitations. First, regarding data bias and universality, while citizen appeals carry inherent reporting biases (e.g., underrepresentation of silent marginalized groups), the observed hierarchical evolution of needs reflects fundamental human cognitive patterns that likely transcend this specific dataset. Future research could validate these patterns across diverse geographic contexts. Second, regarding context specificity, although Beijing possesses distinct governance characteristics, its stark urbanization gradient serves as a representative proxy for global megacities. This suggests that the "resilience perception gap" is not merely a local artifact but a generalized challenge for high-density urban systems. Third, regarding causal inference, our machine learning framework identifies drivers and feature importance, however, given the observational nature of the natural experiment, these findings establish spatiotemporal associations rather than strict causality. Finally, our definition of physical recovery relies on metrics of quantity rather than quality. Consequently, the observed gap captures psychological lags and unmeasured functional degradations invisible to sensors, highlighting the need for future metrics that integrate service experience.

Methods

Perceived and Physical City Resilience

For each community, Perceived City Resilience is defined as the ratio of residents whose service requests were resolved (via municipal interventions) to the total affected population. This metric reflects the governmental responsiveness in addressing post-disaster unmet needs, serving as a proxy for citizen-centric recovery perception. We use anonymized geotagged resident appeals and municipal feedback resolution records, comprising 336,928 unique cases that track post-disaster needs and recovery satisfaction. Each piece of data/case is structured through analytical dimensions: *1) Temporal Context:* precise timestamps of request submissions and resolution completions allow

the chronological analysis of governmental responsiveness for human perception. *2) Appeal and Source:* Records describe residents' unmet needs, including infrastructure failures, resource shortages, and other post-disaster challenges. These are collected via multiple reporting channels such as municipal hotlines and social media platforms (e.g., Weibo/WeChat). *3) Operational Response:* Entries track the complete chain of service delivery, covering departmental workflows, personnel deployment, infrastructure restoration timelines, and resolution status (pending/in-progress/resolved). *4) Spatial Precision:* Each entry is geotagged at street-level precision (latitude/longitude), enabling detailed spatial analyses of disaster impact and recovery progress.

For each community, Physical City Resilience quantifies the proportion of the population with restored access to critical services (e.g., power, water), calculated by aggregating service areas of operational facilities within demographic boundaries. This metric represents the physical restoration progress, measured through infrastructure service capacity recovery. We use IoT-monitored infrastructure status reports and GIS-based service area modeling. Each data is structured through four dimensions: *1) Source:* daily operational status reports from 16 categories of critical infrastructure (power/water/sewage/transportation networks). *2) Temporal Resolution:* damage assessments are collected through IoT sensor networks and manual reports, with recovery progress monitored through automated daily system audits. *3) Spatial Dynamics:* dynamic service area modeling via ArcGIS Network Analyst calculates the coverage ratio by determining the population served by each facility based on administrative boundaries and local demographics. *4) Recovery Trajectory Clustering and Service Gap Identification:* datasets integrate physical facility conditions, social media reports, and municipal recovery plans. Spatial joins in GIS link each facility with demographic profiles of administrative areas. By aligning both metrics to population coverage ratios, we establish a unified scale for cross-dimensional resilience analysis.

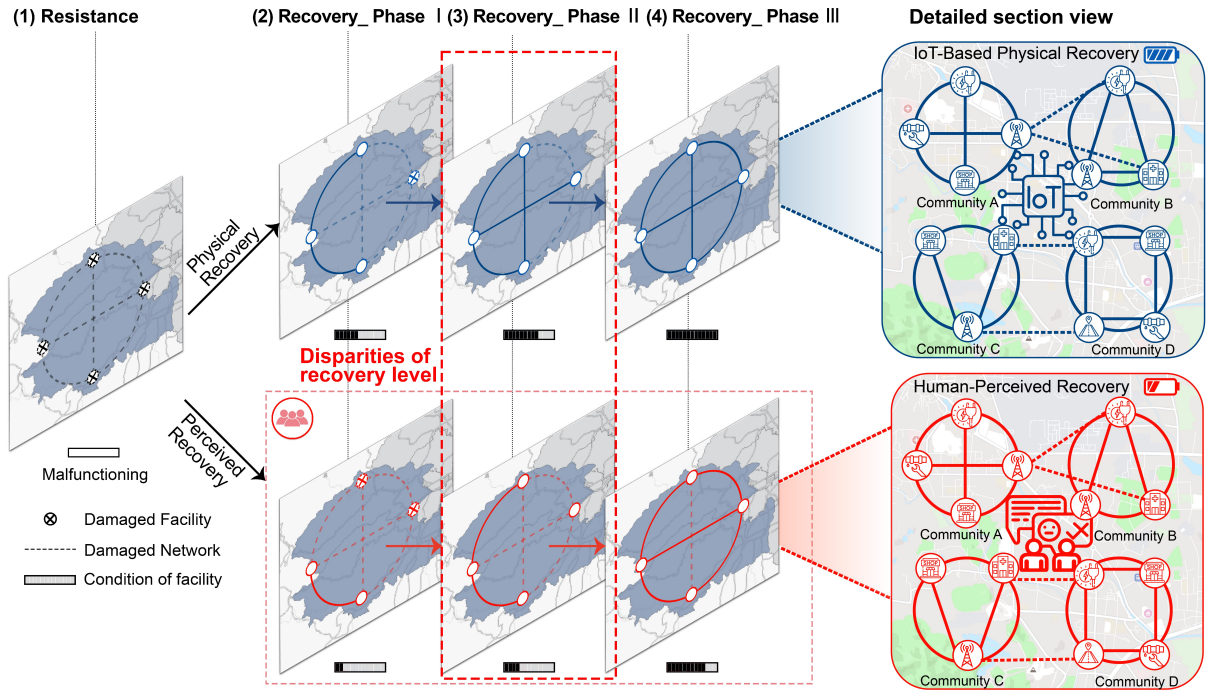

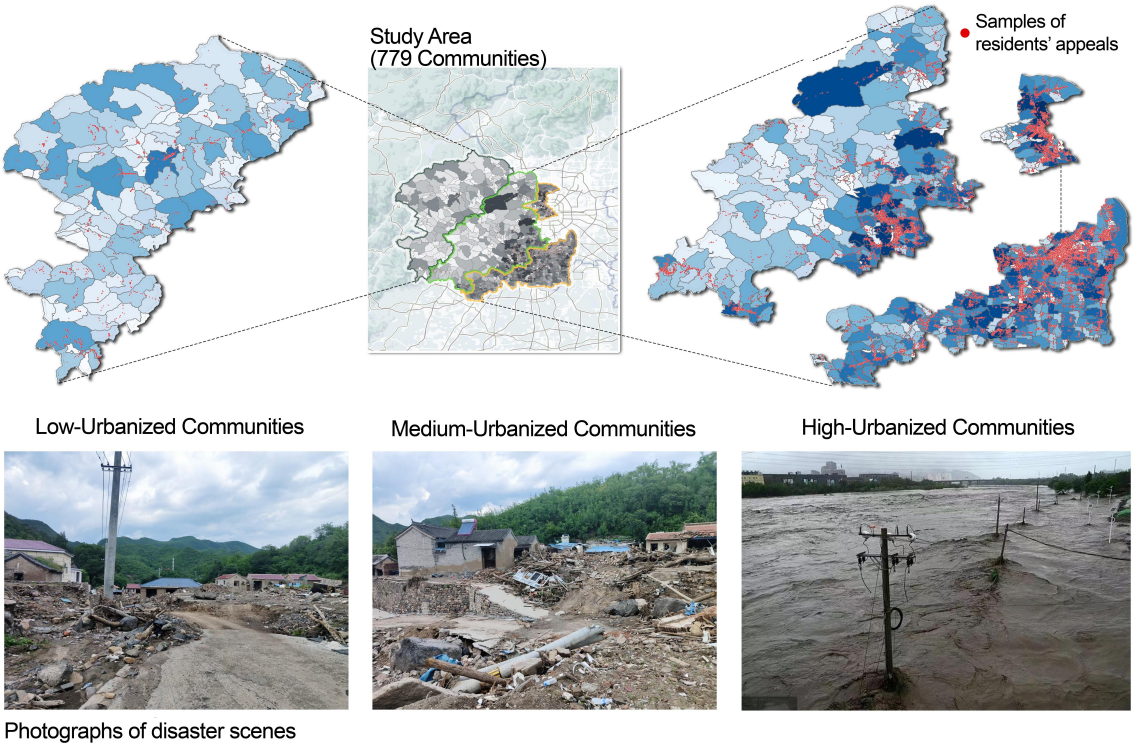

Fig. 8.|Workflow and Surveyed communities of Human Perceived Recovery vs. Physical Recovery. The top row, where the IoT-based physical recovery tracks damaged facilities and infrastructure from an initial disaster state through multiple recovery phases. This part illustrates how cities restore critical services and networks. The lower part emphasizes residents' assessments of whether their needs and well-being are addressed at each stage.

Modeling City Recovery and Assessing Perceived and Physical Resilience

We propose a five-step methodology to assess the discrepancies between perceived and physical recovery following extreme rainstorms. The study covers 779 communities (urban and rural) in a mega-city in China, with a population of 1.7 million, and spans an area of 3,467 km^2. The disaster, recorded as the worst rainstorm in 140 years, caused over 10 billion USD in damages. This research uses Python (version 3.9) and ArcGIS Pro (version 3.2.0) to implement geospatial analyses and machine learning applications.

Step 1: Modeling City Recovery through facility functionality and population service coverage (as illustrated in Fig. 8). *(1) Preparation (Well-functioning Phase):* All facilities and infrastructure networks are assumed to be fully operational before disaster events, establishing a baseline for recovery simulation. Facility functionality is quantified using the population service coverage based on administrative boundaries and local demographic data. *(2) Resistance (Malfunctioning Phase)*. Following the disaster, facilities and networks malfunction, reducing their population service coverage, resulting from infrastructure damage and loss of functionality. (*3) Recovery I-III (Emergency Recovery ->Continued Recovery->Full Recovery).* Recovery begins as the system starts repairing physical damage to the facilities and networks. Recovery Phase I measures emergency physical repairs. The system's recovery is tracked through physical restoration, with functionality improving as facilities are restored. During this phase, recovery continues, but both physical restoration and perceived recovery (the public's satisfaction and trust in the system's functionality) are measured. By Phase III, the physical functionality returns to pre-disaster baseline levels. Our study also introduces disparities in recovery levels across different urban settings (low, medium, and high urbanization levels), highlighting how recovery progresses differently in these communities. The points of interest in these areas are also noted, reflecting the diverse needs and recovery priorities in each community.

Step 2: Specifying human needs indicators for examining perceived-physical recovery based on Latent Dirichlet Allocation (LDA) Topic Modeling. This study applied LDA to categorize residents' needs metrics, refined these needs index through post-disaster field surveys, and verified them through a two-round Delphi study. The LDA topic generation procedure encompasses the following steps: For each resident's appeal document d within the corpus, select a distribution $\theta_d \sim Dirichlet(\alpha)$, $d \in \{1,...,D\}$. For each word in the document d, determine $z \sim multinomial(\theta_d)$. For each topic $u \in \{1,...,U\}$, select a distribution $\phi k \sim Dirichlet(\beta)$. The probability and relative weight of each word in the need topic are as follows.

$$p(w|d) = \sum_{u=1}^{u} p(w|z = u, \phi_u) p(z = u|\theta_d \mid u \in U) \quad (1)$$

Here, w represents the frequency of an element in the resident's appeal document d, z denotes the need k. θ_d and ϕ_k indicate the Dirichlet distribution with parameters α and β, respectively.

Step 3: Quantify perceived-physical city resilience using performance curves. To assess city resilience, we employed serviceability metrics to track both perceived and physical performance curves. For perceived performance curve, we quantified accumulated unmet needs with temporally normalized recovery rates. Specifically, we used a needs-fulfillment metric as a proxy for perceived recovery, where performance curves chart the restoration of unmet needs over time. By monitoring the emergence and resolution of these needs, we obtain continuous insights into recovery dynamics (Equation 2). The priority of each need is defined by calculating the proportion of its unmet volume relative to the total unmet needs. The priority of each need is determined by calculating the proportion of its unmet volume relative to the total unmet demand, thereby assigning greater weight to needs with higher unmet volumes (Equation 3). For each need u, the weight adjusts dynamically over day n as unmet demand evolves, which serves as a special innovation in our framework.

$$Accumulated_{u,d_n} = \sum_{d_n=t_0}^{d_n=t} V_{appeal(u,d_n)} - V_{finish(u,d_n)} \ (\forall_p \in p_u \mid u \in U) \quad (2)$$

$$Weight_{u,d_n} = \frac{Accumulated_{u,d_n}}{\sum_{d_n=t_0}^{d_n=t} Accumulated_{u,d_n}} \ (\forall_p \in p_u \mid u \in U) \quad (3)$$

Where $\mathrm{Accumulated}_{\mathrm{u,d_n}}$ is the total volume of unmet need u on *day n,* and $\mathrm{p_u}$ is the set of all all-community locations with unmet need u. For each unmet need u, the fulfillment level can be represented by $\widetilde{\mathrm{Accumulated}}_{\mathrm{u,d_n}}$ (inversely normalized to reflect the proportion of unmet demand).

For both perceived and physical performance curves, we integrate accumulated service capabilities with time-normalized recovery rates.

$$Perceived_{u,d_n} = Weight_{u,d_n} \ \widetilde{Accumulated}_{u,d_n} \quad (4)$$

$$Physical_{u,d_n} = Weight_{u,d_n} \ Functionality_{u,d_n} \quad (5)$$

Each dimension of resilience is quantified by evaluating the integral of weighted performance over time. The overall urban resilience is then derived by aggregating these perceived and physical measures. To capture both the magnitude of the event (e.g., peak or maximum amplitude of unmet demand) and the duration of recovery (i.e., days until post-event equilibrium), we introduce a new

resilience metric, which the integration of expected and actual performance curves offers a overall resilience assessment. Specifically, we compute the area above or below the recovery curve as:

$$R = \frac{\int_{d_n=t_0}^{d_n=t} Actual_{u,d_n}}{\int_{d_n=t_0}^{d_n=t} Expected_{u,d_n}} (\text{actual}_{\text{u,d}_\text{n}} : \text{Perceived}_{\text{u,d}_\text{n}}; \text{Physical}_{\text{u,d}_\text{n}}) \quad (6)$$

where *R* represents the resilience, reflecting how quickly and effectively the system returns to its expected level following the disruptive event.

Step 4: Quantifying Perceived–Physical Resilience Disparities and Conducting Spatial Analysis via a Machine Learning Model. We quantified perceived–physical recovery disparities at different disaster stages by calculating the integrated area between each dimension's performance curves. Larger integrals indicate greater divergence between residents' subjective perceptions of recovery (linked to unmet needs) and observed physical progress, revealing how these gaps evolve over time:

$$Disparity\ (Phase\ i) = \frac{\int_{d_n=t_0}^{d_n=t_i} \sum_{u=1}^{U} Perceived_{u,d_n} - \int_{d_n=t_0}^{d_n=t_i} \sum_{u=1}^{U} Physical_{u,d_n}}{t_i - t_0} (\forall_{\text{p}} \in \text{p}_\text{u} \mid \text{Phase i} \in \text{t}_\text{i} - \text{t}_0) \quad (7)$$

These disparities served as the dependent variables in a geographically weighted random forest model to account for spatial heterogeneity in unmet needs. We incorporated precipitation intensity, terrain slope, river network density, vegetation coverage, impervious surfaces ratio, public service index, commercial service density, population density, economic activity index as explanatory variables. For each observation, this model calibrates a localized non-linear function by assigning spatial weights to neighboring observations according to geographic distance:

$$Y_i = \alpha((u_i, v_i), x_i) + e_i \quad (8)$$

Where Y_i is the predicted recovery disparity at location i. $\alpha((\text{u}_\text{i}, \text{v}_\text{i}), \text{x}_\text{i})$ represents the localized non-linear effect of each explanatory variable. We used an adaptive kernel to determine the optimal bandwidth for spatial weighting, enabling a refined analysis of local recovery dynamics.

Step 5: Comparing Actual and Expected Resilience as a Social Benchmark for each need u. We define another disparity based on each need *u* measure to indicate the gap between the modeled expected recovery trajectory and the actual observed recovery (including perceived and physical resilience). Then we can analyze recovery patterns of residents' needs that influences the perceived–physical resilience disparities:

$$Disparity_{u,d_n} = Expected_{u,d_n} - Actual_{u,d_n}(\text{Actual}_{\text{u,d}_\text{n}}: \text{Perceived}_{\text{u,d}_\text{n}}; \text{Physical}_{\text{u,d}_\text{n}}) \quad (9)$$

$$Expected_{u,d_n} = e^{-\rho*(TL_k - t_k)} = \frac{e^{\rho*t_k}}{e^{\rho*TL_k}} \quad (10)$$

Expected$_{\text{u,d}_\text{n}}$ is the expected performance for each need u, TL_u represents residents' tolerance time of the need, t_u is the interruption time of need u. In this exponential function, $\rho \geq 0$ is a rate parameter indicating how quickly the recovery curve approaches its upper limit. A smaller TL_u is assigned to needs that require swift but possibly partial restoration (for example, emergency supplies). By comparing Actual$_{\text{u,d}_\text{n}}$ with Expected$_{\text{u,d}_\text{n}}$, one can identify potential gaps or overshoots. If perceived recovery lags behind physical restoration but surpass the expected recovery, residents may still feel certain about reliability even though essential systems appear malfunction. Conversely, if perceived recovery exceeds the physical level but lags behind expected recovery, resources might be shifted away too soon, leaving unresolved vulnerabilities.

References

1. Tanner, T. *et al.* Livelihood resilience in the face of climate change. *Nat. Clim. Change* **5**, 23–26 (2015).
2. Kontokosta, C. E., Hong, B. & Bonczak, B. J. Socio-spatial inequality and the effects of density on COVID-19 transmission in US cities. *Nat. Cities* **1**, 83–93 (2024).
3. He, C. *et al.* The overlooked health impacts of extreme rainfall exposure in 30 east asian cities. *Nat. Sustainability* **7**, 423–431 (2024).
4. Chaigneau, T. *et al.* Reconciling well-being and resilience for sustainable development. *Nat. Sustainability* **5**, 287–293 (2021).
5. Hong, B., Bonczak, B. J., Gupta, A. & Kontokosta, C. E. Measuring inequality in community resilience to natural disasters using large-scale mobility data. *Nat. Commun.* **12**, 1870 (2021).
6. Markhvida, M., Walsh, B., Hallegatte, S. & Baker, J. Quantification of disaster impacts through household well-being losses. *Nat. Sustainability* **3**, 538–547 (2020).
7. Jones, L., A. Constas, M., Matthews, N. & Verkaart, S. Advancing resilience measurement. *Nat. Sustainability* **4**, 288–289 (2021).
8. Logan, T. M., Aven, T., Guikema, S. D. & Flage, R. Risk science offers an integrated approach to resilience. *Nat Sustain* **5**, 741–748 (2022).
9. Yi, F., Deng, D. & Zhang, Y. Collaboration of top-down and bottom-up approaches in the post-disaster housing reconstruction: evaluating the cases in yushu qinghai-tibet plateau of China from resilience perspective. *Land Use Policy* **99**, 104932 (2020).
10. MacArthur, B. D., Dorobantu, C. L. & Margetts, H. Z. Resilient government requires data science reform. *Nat. Hum. Behav.* **6**, 1035–1037 (2022).

11. Pan, S., Zhao, Z., Lim, H. W. & Li, N. Restored Quality of Life-based approach (REQUALIFE) for urban seismic resilience assessment: Case study. *International Journal of Disaster Risk Reduction* **79**, 103170 (2022).

12. Zhao, Z. *et al.* A seismic emergency performance optimization model for infrastructure systems under demand differences: A case study in China. *Earthquake Engineering and Resilience* **1**, 196–210 (2022).

13. Elmqvist, T. *et al.* Sustainability and resilience for transformation in the urban century. *Nat. Sustainability* **2**, 267–273 (2019).

14. Baum, C. M., Fritz, L., Low, S. & Sovacool, B. K. Public perceptions and support of climate intervention technologies across the global north and global south. *Nat. Commun.* **15**, 2060 (2024).

15. Bustillos Ardaya, A., Evers, M. & Ribbe, L. Participatory approaches for disaster risk governance? Exploring participatory mechanisms and mapping to close the communication gap between population living in flood risk areas and authorities in nova friburgo municipality, RJ, brazil. *Land Use Policy* **88**, 104103 (2019).

16. Zhao, Z., Li, Z., Tong, R., Gu, T. & Fang, D. Unveiling the spatial heterogeneity of factors influencing physical and perceived recovery disparities under extreme rainstorms: a geographically weighted machine learning approach. *Sustainable Cities Soc.* **118**, 106023 (2025).

17. Dargin, J. S. & Mostafavi, A. Human-centric infrastructure resilience: Uncovering well-being risk disparity due to infrastructure disruptions in disasters. *PLoS ONE* **15**, e0234381 (2020).

18. Zhao, Z., Zhou, X., Zheng, Y., Meng, T. & Fang, D. Enhancing infrastructural dynamic responses to critical residents' needs for urban resilience through machine learning and hypernetwork analysis. *Sustainable Cities Soc.* **106**, 105366 (2024).

19. Pan, S., Zhao, Z., Lim, H. W., Li, N. & Fang, D. Restored quality of life-based approach (REQUALIFE) for urban seismic resilience assessment: Quantitative method. *International Journal of Disaster Risk Reduction* **79**, 103169 (2022).

20. Yin, J. *et al.* Strategic storm flood evacuation planning for large coastal cities enables more effective transfer of elderly populations. *Nat. Water* **2**, 274–284 (2024).

21. Maslow, A. H. A theory of human motivation. Psychological review **50**, 370–396 (1943).

22. Yoshitsugu Hayashi & Yasuhiro Suzuki. *Resilience for Empowering the Regions—National Grand Design Making Good Use of Traditional Knowledge and Big Data*. (Tsinghua University Press, 2016).

23. Zhao, Z., Zhou, X., Asce, S. M. & Lin, Z. A resident-centric framework for postdisaster infrastructure recovery: characterizing hierarchical needs and fulfillment cycles to assess urban resilience. *Journal of Management in Engineering* **41**, 04025003 (2025).

24. Delilah Roque, A., Pijawka, D. & Wutich, A. The role of social capital in resiliency: disaster recovery in Puerto Rico. *Risk Hazards Crisis Public Policy* **11**, 204–235 (2020).

25. Li, H., Han, Y., Wang, X. & Li, Z. Risk perception and resilience assessment of flood disasters based on social media big data. *Int. J. Disaster Risk Reduct.* **101**, 104249 (2024).

26. Hong, B., Bonczak, B. J., Gupta, A. & Kontokosta, C. E. Measuring inequality in community resilience to natural disasters using large-scale mobility data. *Nat. Commun.* **12**, 1870 (2021).

27. Liu, W., Gerber, E., Jung, S. & Agrawal, A. The role of human and social capital in earthquake recovery in Nepal. *Nat. Sustainability* **5**, 167–173 (2021).

28. Christensen, J., Aarøe, L., Baekgaard, M., Herd, P. & Moynihan, D. P. Human capital and administrative burden: the role of cognitive resources in citizen-state interactions. *Public Administration Review* **80**, 127–136 (2020).

29. Haushofer, J. & Fehr, E. On the psychology of poverty. *Science* **344**, 862–867 (2014).

30. Mani, A., Mullainathan, S., Shafir, E. & Zhao, J. Poverty impedes cognitive function. *Science* **341**, 976–980 (2013).

31. Barretto-García, M. *et al.* Individual risk attitudes arise from noise in neurocognitive magnitude representations. *Nat. Hum. Behav.* **7**, 1551–1567 (2023).

32. Tan, J., Lin, L. & Cao, T. How do psychological factors influence disaster preparedness? Evidence from disaster-stricken mountainous areas of China. *Disaster Med. Public Health Prep.* **18**, e339 (2024).

33. León, J. A., Ordaz, M., Haddad, E. & Araújo, I. F. Risk caused by the propagation of earthquake losses through the economy. *Nat Commun* **13**, 2908 (2022).

34. Yabe, T., Rao, P. S. C. & Ukkusuri, S. V. Regional differences in resilience of social and physical systems: case study of Puerto Rico after hurricane maria. *Environ. Plann. B: Urban Anal. City Sci.* **48**, 1042–1057 (2021).

35. Sanders, B. F. *et al.* Large and inequitable flood risks in los angeles, california. *Nat. Sustainability* **6**, 47–57 (2022).

36. Frankenberg, E., Sumantri, C. & Thomas, D. Effects of a natural disaster on mortality risks over the longer term. *Nat. Sustainability* **3**, 614–619 (2020).

37. Rachunok, B. & Nateghi, R. Overemphasis on recovery inhibits community transformation and creates resilience traps. *Nat. Commun.* **12**, 7331 (2021).

38. Smiley, K. T. *et al.* Social inequalities in climate change-attributed impacts of Hurricane Harvey. *Nat Commun* **13**, 3418 (2022).

39. Moghadas, M., Asadzadeh, A., Vafeidis, A., Fekete, A. & Kötter, T. A multi-criteria approach for assessing urban flood resilience in Tehran, iran. *Int. J. Disaster Risk Reduct.* **35**, 101069 (2019).

40. Norris, F. H., Stevens, S. P., Pfefferbaum, B., Wyche, K. F. & Pfefferbaum, R. L. Community resilience as a metaphor, theory, set of capacities, and strategy for disaster readiness. *Am. J. Community Psychol.* **41**, 127–150 (2008).

41. Zhai, W., Hu, W., Yuan, Z. & Li, Y. Examining disaster resilience perception of social media users during the billion-dollar hurricanes. *Nat. Hazard.* **120**, 701–727 (2024).

42. Kephart, J. L. Social disparities in neighborhood flood exposure in 44,698 urban neighborhoods in latin america. 1-8 (2025).

43. Pfefferbaum, B., Van Horn, R. L. & Pfefferbaum, R. L. A conceptual framework to enhance community resilience using social capital. *Clin. Soc. Work J.* **45**, 102–110 (2017).

44. Zhao, Z., Li, Z., Wang, T., Lin., Z. & Fang, D. Post-disaster recovery planning for infrastructure systems based on residents' needs: a hypernetwork approach. *Int. J. Disaster Risk Reduct.* **118,** 105258 (2025).

631 45. Straub, A. M., Gray, B. J., Ritchie, L. A. & Gill, D. A. Cultivating disaster resilience in rural
632 oklahoma: community disenfranchisement and relational aspects of social capital. *J. Rural*
633 *Stud.* **73**, 105–113 (2020).

634 46. Opabola, E. A. & Galasso, C. Informing disaster-risk management policies for education
635 infrastructure using scenario-based recovery analyses. *Nat. Commun.* **15**, 325 (2024).

636 47. Mohammadi, N. & Taylor, J. E. Thinking fast and slow in disaster decision-making with smart
637 city digital twins. *Nat. Comput. Sci.* **1**, 771–773 (2021).

638 48. Li, Z., Idziorek, K., Chen, A. & Chen, C. Untapped capacity of place-based peer-to-peer
639 resource sharing for community resilience. *Nature Cities* **2**, 47-57 (2025).

640 49. Yarveysi, F., Alipour, A., Moftakhari, H., Jafarzadegan, K. & Moradkhani, H. Block-level
641 vulnerability assessment reveals disproportionate impacts of natural hazards across the
642 conterminous united states. *Nat. Commun.* **14**, 4222 (2023).

643 50. Winkler, R. L. *et al.* Unequal access to social, environmental and health amenities in US urban
644 parks. *Nat. Cities* **1***,* 861-870 (2024).

645 51. Shah, A. K., Mullainathan, S. & Shafir, E. Some consequences of having too little. *Science* **338**,
646 682–685 (2012).

647 52. Danziger, M. M. & Barabási, A.-L. Recovery coupling in multilayer networks. *Nat. Commun.*
648 **13**, 955 (2022).

649